

Layer-wise Instance Binding for Regional and Occlusion Control in Text-to-Image Diffusion Transformers

Ruidong Chen¹ Yancheng Bai^{2†}, Xuanpu Zhang¹, Jianhao Zeng¹, Lanjun Wang¹,
Dan Song¹, Lei Sun², Xiangxiang Chu², Anan Liu^{1*},
¹Tianjin University, ²Independent Researcher



Figure 1. We propose **LayerBind**, a training-free strategy to empower text-to-image DiT models [3, 39] with regional and occlusion controllability. (Top) Compared to prior methods [52, 53], LayerBind produces customized images that respect the specified spatial layout and occlusion relations without image quality degradation. (Bottom) LayerBind is based on a context-sharing, region-branching strategy. This design inherently enables editable generation, allowing flexible modifications like changing per-region instances or visible orders.

Abstract

Region-instructed layout control in text-to-image generation is highly practical, yet existing methods suffer from limitations: (i) training-based approaches inherit data bias and often degrade image quality, and (ii) current techniques struggle with occlusion order, limiting real-world usability. To address these issues, we propose **LayerBind**. By modeling regional generation as distinct layers and binding them during the generation, our method enables precise regional and occlusion controllability. Our motivation stems from the observation that spatial layout and occlusion are established at a very early denoising stage, suggesting that rearranging the early latent structure is sufficient to modify the final output. Building on this, we structure the scheme into two phases: instance initialization and subsequent se-

mantic nursing. (1) First, leveraging the contextual sharing mechanism in multimodal joint attention, **Layer-wise Instance Initialization** creates per-instance branches that attend to their own regions while anchoring to the shared background. At a designated early step, these branches are fused according to the layer order to form a unified latent with a pre-established layout. (2) Then, **Layer-wise Semantic Nursing** reinforces regional details and maintains the occlusion order via a layer-wise attention enhancement. Specifically, a sequential layered attention path operates alongside the standard global path, with updates composited under a layer-transparency scheduler. LayerBind is training-free and plug-and-play, serving as a regional and occlusion controller across Diffusion Transformers. It also supports editable workflows, allowing for flexible modifications like changing instances or rearranging visible orders. Experimental results demonstrate LayerBind’s effec-

* Corresponding author; † Project lead.

tiveness, highlighting its potential for creative applications.
 Project page: <https://littlefatshiba.github.io/layerbind-page>

1. Introduction

Text-to-Image (T2I) models have advanced rapidly, with Diffusion Transformers (DiTs) [11, 35] emerging as the dominant architecture due to their strong scalability and high-fidelity generation quality. To enhance controllability, region-instructed layout control [8, 27, 53, 58, 59] uses regional cues (e.g., boxes or masks with associated instructions) to dictate instance placement and appearance. This approach is valued for executing user-specified or LLM-parsed layout plans [8, 12, 49] and has garnered widespread research attention. However, most existing methods [27, 28, 36, 58, 59] are designed particularly for U-Net pipelines [11, 38], which are transferred poorly to DiTs, given their substantially different attention mechanisms, tokenization schemes, and model size. Consequently, research on DiT-native layout controllers remains limited.

Existing DiT-native layout controllers primarily follow two directions. First, training-based methods, which fine-tune the DiT model [53] or adopt layout adapters [16, 45, 47]. While these methods can achieve precise layout control, they introduce training data bias, causing image quality degradations (e.g. CreatiLayout [53] in Fig. 1). Second, training-free methods, such as [4, 8, 52], conduct regional prompting to inject semantics into localized regions, often preserving the model’s original generation quality. However, despite both having advantages, they fail to manage object occlusion, and often cause “concept blending”, where semantics from different regions erroneously fuse (Fig. 5). This highlights a critical and shared gap: **achieving robust control over both regional layout and occlusion with high-fidelity generation in DiTs** remains an unsolved problem.

To address these limitations, we propose **LayerBind**, a training-free controller enabling precise regional and occlusion control for DiTs. Our approach is motivated by a key observation regarding the model’s denoising dynamics: the foundational layout is rigidly established at a very early denoising step [24, 30, 32, 37] (Fig. 2a), and through rearranging this early latent structure, we can directly modify the final layout and occlusion (Fig. 2b). This leads to our core motivation: **effective layout control should align with the model’s intrinsic denoising dynamics**, rather than countering them at temporally misaligned stages. LayerBind implements this principle by decoupling the region-instructed layout control into two sequential phases (Fig. 2c): (1) **Layer-wise Instance Initialization**, an early-stage process to initialize instances and define layout and occlusion, and (2) **Layer-wise Semantic Nursing**, a subsequent phase to refine instance details while maintaining occlusion integrity.

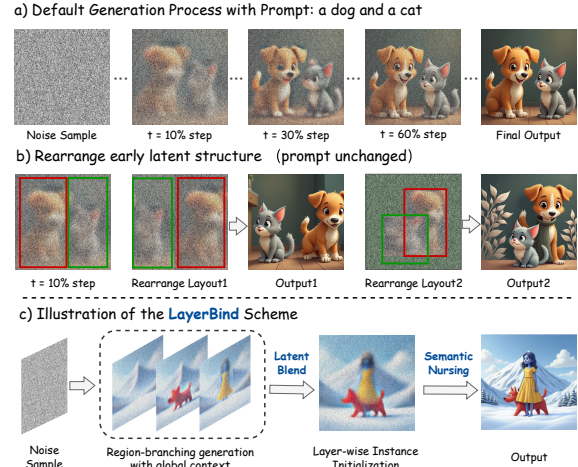


Figure 2. (a, b) Observation: simply rearranging the latent structure at an early step directly manipulates the final spatial layout and occlusion order. (c) Our LayerBind scheme: initializing the instance layout first, then conducting semantic nursing for instance detail while maintaining layout and occlusions.

LayerBind implements this two-stage design as follows. (1) **Layer-wise Instance Initialization** first creates per-instance branch tokens from the initial latents, corresponding to each specified region. Leveraging the contextual sharing mechanism of multimodal joint-attention (MM-Attention) [11], these branches compute attention independently, allowing them to form distinct instances while adapting the shared background context. At a designated early step, these branches are fused into the global latent according to the desired layer order, either via direct latent merging or by using an optional foreground blend to composite the instances, thereby establishing the initial structured latent. (2) **Layer-wise Semantic Nursing** then takes over after the merge. This stage performs semantic refinement via layer-wise local attention enhancements. In each attention block, a standard global path runs, followed by a sequential layered path that processes each region and its instruction. A layer-transparency scheduler then manages these layered enhancements, ensuring regional semantics and layer relationships are progressively reinforced throughout the subsequent denoising process.

In summary, LayerBind is a training-free and plug-and-play controller that enables precise region and occlusion control for DiTs while preserving generation quality. Furthermore, its region-branching scheme inherently enables an editable generation. This design permits flexible modifications, such as changing per-region objects, altering occlusion order (Fig. 1, Bottom), or even performing composited image editing with any image as background context (Fig. 8). Extensive quantitative and qualitative experiments validate LayerBind’s state-of-the-art performance in complex layout and occlusion control.

2. Related Work

2.1. Layout-to-Image Generation

Layout-to-Image (L2I) generation [6, 7, 9, 28, 36, 43, 58] aims to control the spatial layouts of synthesized images. A further extension, region-instructed L2I [12, 19, 27, 43, 47, 53, 59], incorporates detailed regional information for finer-grained controllability. Early approaches diverged into three categories: (1) Training-based methods [27, 58, 59] that finetune the model on layout inputs; (2) Latent optimization methods [6, 28, 36] that leverage spatial objectives to guide denoising; and (3) Seed-based methods [13, 26, 32] that manipulate the initial noise for object placement.

While these methods performed well on U-Net models (e.g., Stable Diffusion 1.5 [38]), they struggle to adapt to DiT-based architectures, which feature larger parameter counts and fundamentally different attention mechanisms. Consequently, recent efforts have focused on solutions for these newer base models. Recent efforts include training-based adaptations for DiTs [25, 45, 47, 51, 53] and autoregressive models [14, 20], as well as methods leveraging auxiliary modules like depth parsers [60, 61]. More prominently, training-free regional prompting methods [4, 8, 49] leverage the high-fidelity generation of pre-trained DiTs, often using LLMs as layout parsers, to achieve customized generation. However, as discussed in our introduction, these methods struggle with complex spatial relationships, particularly object occlusion. LayerBind builds upon this training-free paradigm, aiming to enhance layout precision and empower the model with robust occlusion control capabilities.

2.2. Layer-wise Image Generation

A distinct line of research, relevant to our “layer-wise” concept, employs explicit image layers to enhance generation. The most common approach [10, 17, 41, 55] involves training models on RGBA decomposed object images, granting them the ability to generate foreground images with transparent backgrounds. Other works utilize pre-composed foregrounds as a prior to guide scene generation [21, 48], or use stored layer-wise memories to preserve unedited regions during multi-step image editing [23].

A method particularly relevant to our task (occlusion control) is LaRender [52]. Inspired by NeRF [33] rendering, working on IterComp [56] and GLIGEN [27] base-model, LaRender replaces standard attention with a layer-ordered object rendering process, thereby explicitly modeling occlusion. However, this approach places stringent demands on its layer-wise prompts, often resulting in missing objects (Fig. 1 and Fig. 5). In contrast, LayerBind’s contextual sharing mechanism ensures each layer remains grounded in a shared background context, achieving more robust and accurate generations.

3. Preliminaries

To introduce LayerBind, this section reviews the relevant preliminaries.

Rectified Flow Model. Mainstream DiTs [3, 11] are based on rectified-flow models [11]. During denoising inference, at time t , denote the data sample as \mathbf{x} and condition as \mathbf{y} , a network predicts a velocity field $v_\theta(\mathbf{x}_t, t | \mathbf{y})$ that transports samples along a linear noise-to-data path. Sampling integrates the ODE using an explicit Euler solver on a linearly spaced timestep grid, yielding the denoising trajectory:

$$\mathbf{x}_{k-1} = \mathbf{x}_k + (t_{k-1} - t_k) v_\theta(\mathbf{x}_k, t_k | \mathbf{y}). \quad (1)$$

This trajectory makes each state the initial condition for all subsequent updates, so simple rearrangements applied early deterministically propagate through the entire trajectory, directly supporting our early-binding motivation for layout and occlusion control.

Multimodal Diffusion Transformers (MM-DiT). Modern DiTs [11] unify textual and visual tokens via a single joint attention operator, computing self-attention over a unified sequence to enable bidirectional context sharing. Let text and image tokens be $T \in \mathbb{R}^{N_T \times d_T}$ and $I \in \mathbb{R}^{N_I \times d_I}$. They are mapped to a shared d -dimensional space to produce queries (Q_T, Q_I), keys (K_T, K_I), and values (V_T, V_I). Joint attention A_{joint} is then calculated by concatenating tokens from both modalities:

$$A_{\text{joint}}(Q, K, V) = \text{Softmax} \left(\frac{[Q_T \oplus Q_I][K_T \oplus K_I]^T}{\sqrt{d}} \right) [V_T \oplus V_I], \quad (2)$$

where \oplus denotes concatenation along the sequence dimension. This formulation allows all tokens to freely attend to each other, enabling powerful cross-modal reasoning.

Localized Attention with Contextual Update. The flexibility of joint attention (Eq. 2) allows for updating local tokens by selectively constructing Q , K , and V , enabling fine-grained information flow [5, 15, 22, 57]. Specifically, given local tokens (T/I_{local}) and context tokens (T/I_{context}), we can update the former using them as queries (Q_{local}), while concatenating both to form keys and values ($K = [K_{\text{local}} \oplus K_{\text{context}}]$, $V = [V_{\text{local}} \oplus V_{\text{context}}]$). With Eq. 2, we define this operation, which we term “**Contextual Attention**” (Fig. 3), as:

$$A_{\text{update}}(Q_{\text{local}}, [K_{\text{local}} \oplus K_{\text{context}}], [V_{\text{local}} \oplus V_{\text{context}}]). \quad (3)$$

To simplify notation and the explanation of proposed LayerBind, we abbreviate this operation as $\hat{e}_{\text{out}} \leftarrow A_{\text{update}}(e_{\text{query}}, e_{\text{context}})$, where e_{context} may be a concatenation of multiple contexts, such that $e_{\text{context}} = [e_{\text{ctx}_1}, e_{\text{ctx}_2}, \dots]$. This functional representation maintains consistency with joint attention and is mathematically equivalent to attention masking [4, 8, 44, 60], yet improves efficiency and clarifies the information flow for local token updates.

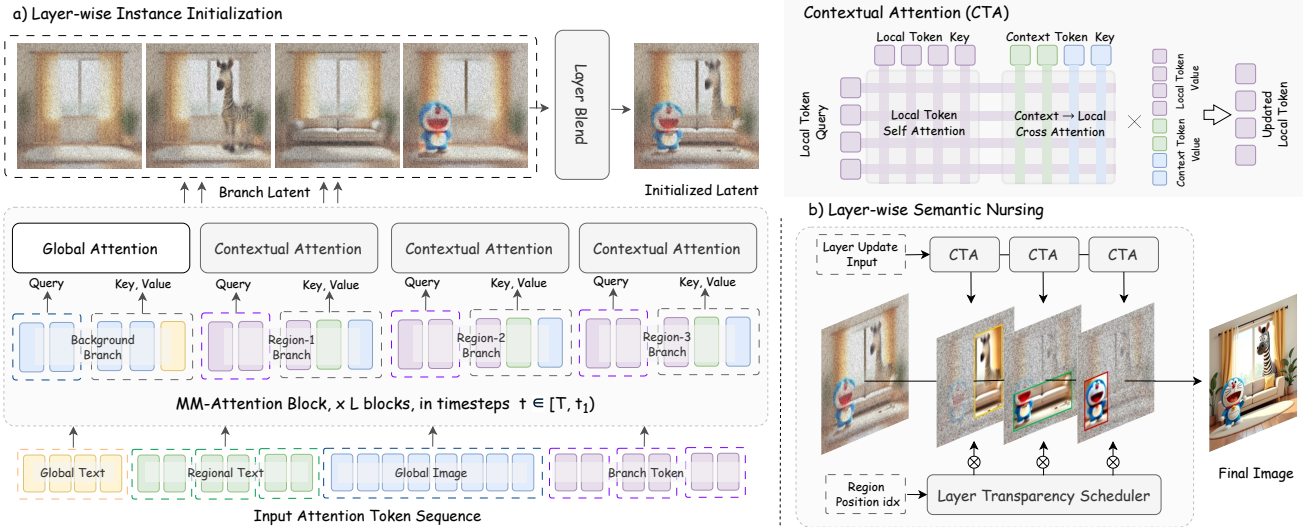


Figure 3. Overview of the LayerBind pipeline. (a) **Layer-wise Instance Initialization** splits early denoising into background and instance branches. Each instance generates independently while sharing background context (via Contextual Attention, CTA, Eq. 3), then they are fused to form the initialized early latent. (b) **Layer-wise Semantic Nursing** reinforces following generation. It conduct layer-wise sequential CTA updates for each region, modulated by a Layer Transparency Scheduler, to refine instance details and maintain occlusions. *Note: For simplicity, only image token updates are visualized; the detailed strategy will be described in the following sections.*

4. Method

4.1. Problem Definition

This study focuses on the task of “*region-instructed layout and occlusion control in DiT models*”. Following prior work on region-instructed layout control [4, 8, 12, 21, 49, 53], the inputs are precisely user-defined or LLM-parsed structured inputs, including: a background prompt (T_{bg}) for the initialization stage, a full scene prompt (T_{scene}) for the subsequent nursing stage, and a set of N layered regional inputs. Each layer i includes a regional prompt ($T_{reg}^{(i)}$) and a corresponding spatial cue ($C^{(i)}$) (e.g., box or mask). The layer index i explicitly defines the occlusion order, from farthest ($i = 1$) to nearest ($i = N$). This cue $C^{(i)}$ corresponds to a set of token indices $idx^{(i)}$ in the DiT token sequence.

Given these inputs, the goal is to generate an image that satisfies three key requirements:

- **Layout & Occlusion:** Strict adherence to the spatial cues $C^{(i)}$ and the **pre-defined** i -th layer occlusion order.
- **Regional Fidelity:** Faithful semantic control for each instance $T_{reg}^{(i)}$ without concept blending.
- **Global Harmony:** High-fidelity quality and coherent composition, preserving the base model’s capabilities.

To meet these requirements, we introduce LayerBind (Fig. 3). Our approach decouples this task into two sequential stages: (1) **Layer-wise Instance Initialization** to first establish the layout and (2) **Layer-wise Semantic Nursing** to subsequently refine details and maintain integrity. The following sections will detail each component.

4.2. Layer-wise Instance Initialization

This stage operates during the initial phase of denoising. Let T be the maximum diffusion timestep (e.g., $T = 1000$) and S be the total number of discrete inference steps. This initialization stage is active for the first η_1 ratio of inference steps. This defines a timestep threshold t_1 , such that this phase runs during the interval $t \in [T, t_1]$. At step t_1 , the branches are fused to form the initialized latent.

Branch Construction. At the initial denoising step $t = T$, we construct each branch $B^{(i)}$ by directly copying from the global latent I at the specified indices:

$$B^{(i)}(t = T) \leftarrow I(t = T)[idx^{(i)}]. \quad (4)$$

Inside each DiT block, these latents (I and $B^{(i)}$) are mapped to their corresponding *embeddings*. As illustrated in Fig. 3(a), the attention blocks operate on four main types: the global image embedding (e_I), the instance branch ($e_B^{(i)}$), the global text ($e_{T_{bg}}$), and the regional text ($e_{T_{reg}^{(i)}}$). Crucially, $e_B^{(i)}$ also inherits the RoPE position embeddings [40] from $e_I[idx^{(i)}]$. Based on the ODE sampling properties (Sec. 3), this shared starting point ensures I and all $B^{(i)}$ share the same underlying noise structure, naturally promoting global consistency even as their semantic paths diverge.

Branch Updates with Contextual Attention. The core of the branch update policy is to create a bidirectional binding between each instance branch $e_B^{(i)}$ and its corresponding regional text $e_{T_{reg}^{(i)}}$, while grounding both in the shared visual background context. We define this background context $e_{I_{bg}}^{(i)}$ as the set of global image tokens excluding the i -th region

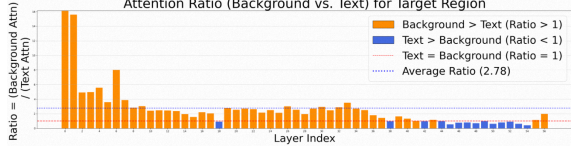


Figure 4. Attention response weights of foreground to background and text across different FLUX [3] layers. We select layer 0 [1, 44] and layers with strong TEXT response for hard instance binding. More analysis is presented in the Appendix A.

(i.e., $e_{I_{bg}}^{(i)} = e_I[\sim idx^{(i)}]$). In parallel, the main embedding e_I and $e_{T_{bg}}$ are updated via standard joint attention. Using the abbreviated Eq. 3, the instance branch update is:

$$\hat{e}_B^{(i)} \leftarrow \mathcal{A}_{\text{update}}(e_B^{(i)}, [e_{I_{bg}}^{(i)}, e_{T_{reg}}^{(i)}]). \quad (5)$$

This allows the branch to adapt to the background content (via $e_{I_{bg}}^{(i)}$), while simultaneously ingesting its semantic guidance (from $e_{T_{reg}}^{(i)}$). Symmetrically, the regional text is also updated to reflect the emerging visual features:

$$\hat{e}_{T_{reg}}^{(i)} \leftarrow \mathcal{A}_{\text{update}}(e_{T_{reg}}^{(i)}, [e_B^{(i)}, e_{I_{bg}}^{(i)}]). \quad (6)$$

Together, Eq. 5 and 6 create a localized feedback loop, refining both the instance’s semantics and its textual guidance simultaneously.

Hard Binding and Reverse Adaptation. A known failure mode during instance initialization is “modality competition” [31], where strong background semantics can overwhelm the weaker regional text signal $e_{T_{reg}}^{(i)}$, causing small objects to be ignored. To mitigate this, we leverage the observation that certain DiT blocks exhibit significantly stronger text responses [1, 44] (Fig. 4). In these “text-dominant” blocks, we employ a hard binding and reverse adaptation policy: First, a hard binding forces the instance branch $e_B^{(i)}$ to update exclusively from itself and its guiding text, severing the link to the background:

$$\hat{e}_B^{(i)} \leftarrow \mathcal{A}_{\text{update}}(e_B^{(i)}, [e_{T_{reg}}^{(i)}]). \quad (7)$$

Second, a reverse adaptation ensures boundary harmony. We force the background regions $e_{I_{bg}}^{(i)}$ to adapt to the branch region $e_B^{(i)}$, and to “emptying out” space for it:

$$\hat{e}_{I_{bg}}^{(i)} \leftarrow \mathcal{A}_{\text{update}}(e_{I_{bg}}^{(i)}, [e_{T_{bg}}, e_B^{(i)}]). \quad (8)$$

In practice, this asymmetric update (Eq. 8) is implemented with a structured attention mask. This strategy ensures small instances receive sufficient textual guidance, while the reverse adaptation maintains a seamless blend between the instance and the scene.

Layer-wise Branch Blending. At the designated blend step t_1 , the N instance branches $B^{(i)}$ are sequentially fused into the global latent I according to the occlusion order. We employ a conditional strategy: unoccupied (bottom) layers are directly merged ($I[idx^{(i)}] \leftarrow B^{(i)}$), while for occluding

(top) layers, an optional foreground alpha mask $\alpha_f^{(i)}$ is estimated (details in Appendix A) to prevent background interference and improve edge quality. These occluding layers are then composited via layer order:

$$I[idx^{(i)}] \leftarrow \alpha_f^{(i)} \cdot B^{(i)} + (1 - \alpha_f^{(i)}) \cdot I[idx^{(i)}]. \quad (9)$$

This yields the final initialized latent with an explicit layout structure.

4.3. Layer-wise Semantic Nursing

Following initialization, this stage maintains the established layout and reinforces regional details during $t \in (t_1, t_2]$, where t_2 is determined by a ratio η_2 of the total inference steps S . This stage utilizes the full scene prompt T_{scene} as the global text condition. In each attention block, a standard global attention $\hat{e}_I^{\text{global}}$ is computed (using e_I and $e_{T_{\text{scene}}}$). In parallel, for each layer i , we compute a local attention enhancement $\hat{e}_{\text{local}}^{(i)}$ for its image region $e_{I_{reg}}^{(i)} = e_I[idx^{(i)}]$, and concurrently update its regional text $e_{T_{reg}}^{(i)}$:

$$\hat{e}_{\text{local}}^{(i)} \leftarrow \mathcal{A}_{\text{update}}(e_{I_{reg}}^{(i)}, [e_{T_{reg}}^{(i)}, e_I]), \quad (10)$$

$$\hat{e}_{T_{reg}}^{(i)} \leftarrow \mathcal{A}_{\text{update}}(e_{T_{reg}}^{(i)}, [e_{I_{reg}}^{(i)}, e_{T_{\text{scene}}}]). \quad (11)$$

To compose the final embedding \hat{e}_I^{out} , these local enhancements $\hat{e}_{\text{local}}^{(i)}$ are sequentially blended onto the global result $\hat{e}_I^{\text{global}}$ via a transparency scheduler. Following the occlusion order (bottom $i = 1$ to top N), we define the base layer as $\hat{e}_{\text{comp}}^{(0)} = \hat{e}_I^{\text{global}}$ and compute the final output via an iterative update:

$$\hat{e}_{\text{comp}}^{(i)} = (1 - \alpha_o^{(i)}) \cdot \hat{e}_{\text{comp}}^{(i-1)} + \alpha_o^{(i)} \cdot \hat{e}_{\text{local}}^{(i)}, \quad (12)$$

where $\alpha_o^{(i)} = \beta \cdot M^{(i)}$, with β is the opacity factor and $M^{(i)}$ is the binary mask for region i . This iterative compositing ensures the semantics of top layers robustly overwrite bottom layers in overlapping regions.

5. Experiments

5.1. Evaluation Settings

Implementation Details. We implement LayerBind on two mainstream DiT models: FLUX.1-dev [3] and SD3.5 Large [39]. For evaluation, we adopt the default generation settings for both models (e.g., inference steps and guidance scale) and apply LayerBind’s two-stage strategy. Specifically, η_1 for Phase 1 (Sec. 4.2) is set to 0.2 for FLUX and 0.25 for SD3.5, while η_2 for Phase 2 (Sec. 4.3) is set to 0.7 by default. The opacity factor β (Eq. 12) is set to 0.7.

Baselines. We compare LayerBind against SOTA methods that accept layouts with regional instructions as input. These include training-based approaches [27, 45, 47, 53] and training-free approaches [4, 8, 52]. Among these,

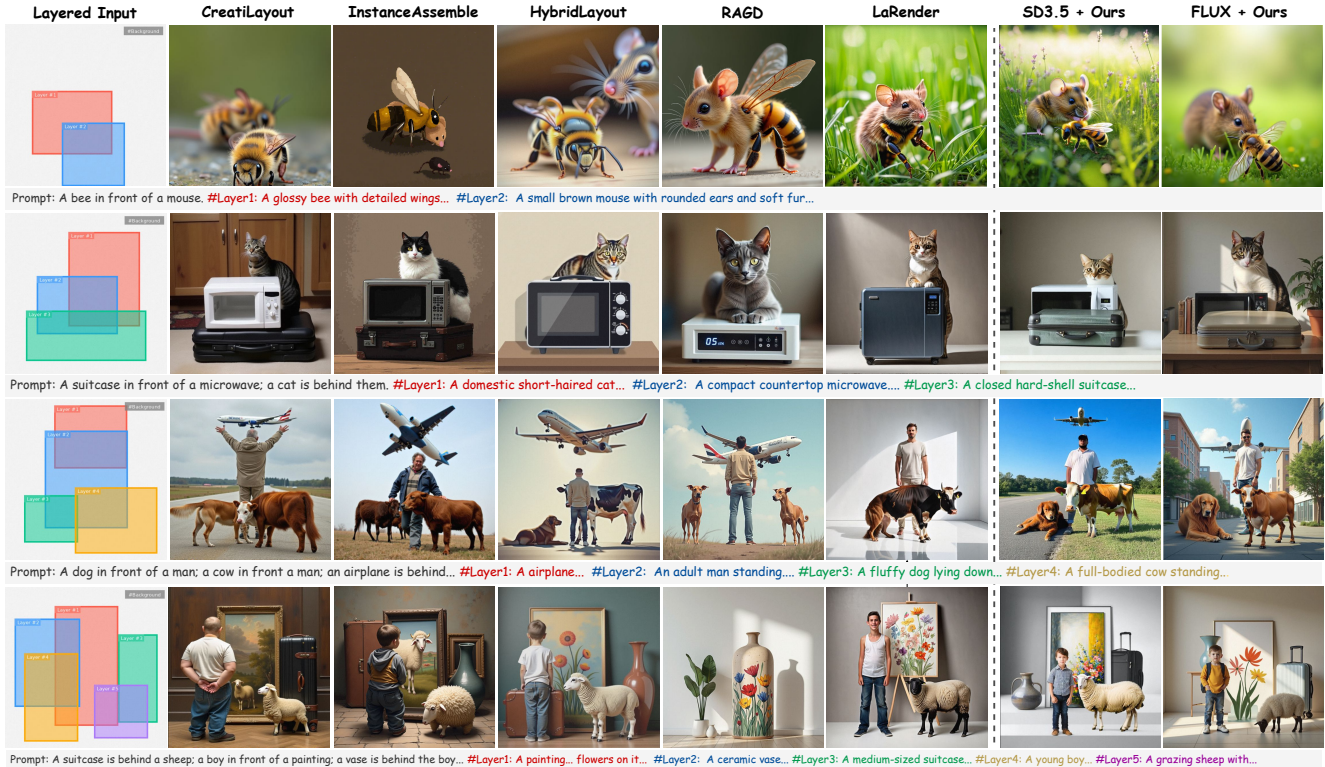


Figure 5. Visualization of occlusion control abilities. Compared to the previous methods, LayerBind achieves more precise layer-wise control, avoiding errors such as instance neglect and concept blending. More visualizations are available in the Appendix F

LaRender is the only method focused on occlusion control; we compare against both its GLIGEN [27] and IterComp [56] implementations. For fair comparison, we use their official implementations with identical seeds and inputs for all generations and evaluations.

Evaluation Benchmarks. To validate the practical application of LayerBind for high-quality customized image generation, we evaluate both occlusion control and T2I alignment tasks. For occlusion control, we use the 3D-spatial subset of T2I-CompBench [18]. To address its limitation to simple two-object relations, we additionally construct BindBench for complex occlusions among 3-5 objects (Appendix B.2). For the general T2I task, we use the attribute bindings, spatial, numeracy, and complex subsets of T2I-CompBench. Lacking publicly released layout annotations, we follow [4, 8, 21, 53] and employ an LLM (e.g., GPT-5-mini [34]) for layout parsing (Appendix B.1).

Metrics. We employ a multi-perspective evaluation for occlusion control: 1) UniDet-Depth [18] measures relative object depth between two objects; 2) CLIP Score (global/local) assesses text-image consistency at both scene and instance levels; 3) O_{VQA} and $L_{Acc/VQA}$, build upon VQAScore [29], quantifies the perceptual score of occlusion relations and layout faithfulness; 4) HPS is reported to assess generation quality [46]. For general T2I alignment, we use the official T2I-CompBench metrics. Please refer to the Ap-

pendix B.3 for full details of our implementation and evaluation protocols.

5.2. Main Results

Qualitative Results Figs. 5 and 6 show qualitative comparisons of LayerBind on occlusion control and T2I alignment tasks, respectively. LayerBind achieves superior alignment with user inputs across both tasks, realizing precise layout and occlusion control while minimizing impact on generation quality. In contrast, while HybridLayout [45] and LaRender [52] similarly adopt a divide-and-conquer strategy for regions, they struggle during region fusion, often leading to concept blending and missing instances. RAGD [8] maintains good image quality, but has difficulty handling complex overlapping layouts. Among training-based methods, CreatiLayout [53] demonstrates the most stable spatial layout capability (likely because it is fully fine-tuned rather than LoRA-based), yet it still fails to handle complex occlusion scenarios. These results underscore the potential of LayerBind as a practical, training-free DiT layout controller for real-world creative applications.

Quantitative Results. Table 1 presents the quantitative results for occlusion control, where LayerBind (on both FLUX and SD3.5) achieves state-of-the-art performance. On T2ICompBench-3D, LayerBind surpasses all competitors in the depth-occlusion metric (UniDet), demon-

Method	Model	Training-free	T2ICompBench-3D [18]					BindBench (Ours)					Inference Speed (s)	
			UniDet \uparrow	CLIP $_G$ \uparrow	CLIP $_L$ \uparrow	O V_{QA} \uparrow	HPS \uparrow	CLIP $_G$ \uparrow	CLIP $_L$ \uparrow	L $_{Acc}$ \uparrow	L $_{VQA}$ \uparrow	O V_{QA} \uparrow		HPS \uparrow
	SD3.5	-	40.06	34.00	-	40.54	28.37	36.33	-	-	-	23.06	30.93	20.96
	FLUX	-	37.97	33.17	-	37.56	29.66	36.08	-	-	-	18.86	30.98	23.12
InstanceDiffusion [43]	SD-2.1	\times	41.53	33.02	28.37	44.73	26.42	35.55	27.71	76.46	40.63	24.09	26.20	16.71 (+308%)
GLIGEN-XL [27]	SD-XL	\times	35.13	33.13	26.97	41.22	26.00	35.03	25.85	74.36	25.32	24.43	26.29	10.52 (+4%)
CreatiLayout* [53]	FLUX	\times	39.37	33.67	27.79	57.03	27.38	36.28	26.60	85.18	40.99	43.62	28.73	16.75 (+148%)
HybridLayout [45]	FLUX	\times	41.33	32.85	26.97	47.55	26.43	35.45	26.14	78.30	43.45	34.10	29.20	78.75 (+240%)
InsAssem [47]	FLUX	\times	31.45	32.29	25.97	40.66	25.37	34.94	25.08	67.24	27.43	30.21	26.42	24.86 (+7%)
CreatiDesign [54]	FLUX	\times	41.00	33.80	24.58	38.60	28.56	36.34	23.01	61.12	25.59	26.26	29.79	75.05 (+224%)
RAGD [8]	FLUX	\checkmark	30.13	32.21	27.61	31.22	26.64	30.43	26.97	36.61	20.81	1.82	22.80	62.14 (+168%)
LaRender [52]	GLIGEN	\checkmark	39.41	32.40	27.52	41.95	25.73	34.30	27.18	60.52	38.53	27.24	25.83	12.49 (+23%)
LaRender [52]	IterComp	\checkmark	37.52	33.14	27.85	35.96	27.37	32.47	25.77	60.52	42.62	17.72	26.27	13.10 (+29%)
LayerBind (Ours)	SD3.5	\checkmark	41.37	33.02	<u>28.49</u>	65.78	<u>28.36</u>	35.01	<u>27.25</u>	<u>87.57</u>	<u>59.73</u>	<u>48.03</u>	29.03	29.39 (+40%)
LayerBind (Ours)	FLUX	\checkmark	44.97	33.12	28.54	59.49	28.25	35.72	27.86	92.18	64.81	52.55	29.66	30.11 (+30%)

Table 1. Quantitative comparison for occlusion control, measuring: depth relationship (UniDet), T2I alignment (CLIP-G/L), Layout alignment (L $_{Acc}/V_{QA}$), occlusion perception score (O V_{QA}), and image quality (HPS). Inference speed includes the percentage of overhead introduced by the controller relative to the base model. * evaluated at 512x512 resolution; all other methods are at 1024x1024.

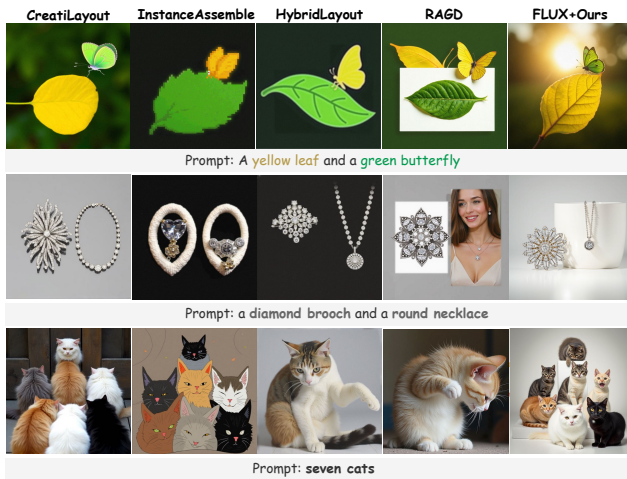


Figure 6. Visualization results on T2I alignment evaluations. LayerBind can serve as a plug-and-play layout controller for improving T2I alignment ability without quality degradation.

	Attribute Binding			Spatial	Numeracy	Complex
	Color	Shape	Texture			
FLUX [3]	77.53	60.16	69.64	39.09	59.81	37.01
CreatiLayout [53]	76.94	59.92	73.45	60.33	71.51	37.45
InstanceAssemble [47]	71.64	55.13	62.15	<u>64.38</u>	56.90	38.33
HybridLayout [45]	<u>84.15</u>	68.82	77.31	63.39	64.57	40.15
RAGD [8]	80.39	60.16	70.85	51.93	53.76	43.77
LayerBind+FLUX (Ours)	84.80	<u>66.48</u>	<u>75.69</u>	70.63	<u>70.93</u>	<u>41.43</u>

Table 2. The quantitative evaluation results of T2I alignment tasks.

strating its ability to generate more natural scene depth. LayerBind’s VQA Score is also notably high across both benchmarks. This advantage is most pronounced on our challenging BindBench, where the performance of most methods degrades sharply, while LayerBind remains robust, proving its reliability in handling complex occlusions. Furthermore, LayerBind attains the highest HPS score, confirming it best preserves image quality. Regarding inference speed, LayerBind’s efficient local attention mechanism is significantly faster than other region-partitioned generation methods (e.g., RAGD [8], HybridLayout [45]).

HB	LSN	CLIP $_G$ \uparrow	CLIP $_L$ \uparrow	VQAScore \uparrow	HPS \uparrow
\times	\times	34.95	26.82	38.36	28.27
\times	\checkmark	34.73	26.90	43.65	28.64
\checkmark	\times	35.78	27.80	50.98	29.64
\checkmark	\checkmark	35.72	27.86	52.55	29.66

Table 3. The quantitative ablation results of applying Hard Binding (Sec. 4.2, HB) and Layer-wise Semantic Nursing (Sec. 4.3, LSN) on BindBench dataset.



Figure 7. Visualization of effect of Hard Binding. It prevents instances from being ignored due to modality competition [31].

Additionally, Table 2 shows the T2I alignment results. Beyond basic attribute binding tasks, LayerBind’s mechanism enables superior performance on difficult Numeracy and Complex tasks, significantly outperforming all existing methods. This indicates that LayerBind is practical not only in occlusion control but also in general T2I generation.

5.3. Ablation Analysis

Module Effectiveness. Table 3 presents the ablation results for our core components on BindBench (using $\eta_1 = 0.2$). The results show that Hard Binding (HB) plays a decisive role in the overall occlusion success rate (VQAScore). Layer-wise Semantic Nursing (LSN) primarily refines regional details while also improving image quality. Fig. 7 illustrates the qualitative impact of HB, which is critical in two scenarios: (1) small objects that are otherwise ignored by global attention, and (2) objects visually similar to the background that fail semantic initialization. Overall, HB strengthens local semantic injection, thereby improving



Figure 8. Applications. Top) As also shown in Fig.1, LayerBind supports flexible occlusion control and instance modifications. Bottom) Treat an original generation as background context and branching edit instructions. LayerBind also achieves composited image edits.

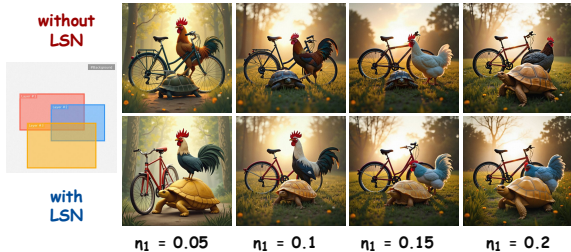


Figure 9. Visualization of effects of different η_1 with LSN strategy. To illustrate the details refinement of LSN, we add color attributes to each region (e.g., golden turtle, blue chicken, red bicycle).

both the instance initialization and the final result. **Effects of different η_1 with LSN.** As shown in Fig. 9, the two phases play complementary roles. First, η_1 controls the structural initialization: the top row (without LSN) demonstrates that a higher η_1 is required to establish the correct structure. The effectiveness of LSN is twofold: it helps maintain the layout and occlusions, and strengthens regional details. The bottom row demonstrates that LSN successfully injects the correct color attributes even when the initial structure is poor. Therefore, LSN serves as a complementary bridge. We can use a moderate η_1 to establish structure, avoiding the instance-background over-decoupling caused by an overly high η_1 (see Appendix C), while LSN ensures the refinement of semantic details, guaranteeing overall harmony.

5.4. Applications

As illustrated in Fig. 1 and Fig. 8, LayerBind’s region-branching mechanism supports flexible applications. First, for layout and occlusion-control tasks, LayerBind serves as a **flexible layout controller** for precise regional-aware generation (Fig. 5, 6). Furthermore, LayerBind’s decoupling of the background and instance generation processes

allows the initialization phase to act as a “shared memory” for the generation, enabling flexible operations such as **instance modifications** (Fig. 1) and **occlusion order modifications** (Fig. 8), all while maintaining consistency in unaffected regions. This inherent editability also extends to **composited image editing** (Fig. 8). For example, a standard generation trajectory (initialized from the same noise or obtained via inversion [42]) can serve as the background context. LayerBind can then process regional edit instructions in separate branches and merge them back into the original trajectory. This enables a powerful, multi-instruction editing capability that preserves irrelevant content, a promising application for interactive content creation. In summary, LayerBind is highly extensible, and we discuss its more applications in Appendix D.

6. Conclusion and Limitations

We propose **LayerBind**, a training-free regional and occlusion controller for text-to-image DiTs. LayerBind decouples the task into two stages: Layer-wise Instance Initialization to establish an early latent with pre-defined layout and occlusion, and Layer-wise Semantic Nursing to further refine details and maintain layouts. Extensive experiments validate LayerBind’s superior performance in complex occlusion control and general T2I alignment tasks, along with application analysis, showing its potential for interactive image customization and image editing applications.

Limitations. Despite its superior performance, LayerBind has certain limitations. For example, some cases exhibit incomplete object generation, instance-background over-decoupling, or poor adherence to unreasonable layouts. We showcase these failure cases in Appendix E and discuss potential solutions for repair, in order to provide a more comprehensive reference for future work.

References

- [1] Omri Avrahami, Or Patashnik, Ohad Fried, Egor Nemchinov, Kfir Aberman, Dani Lischinski, and Daniel Cohen-Or. Stable flow: Vital layers for training-free image editing. In *Proceedings of the Computer Vision and Pattern Recognition Conference*, pages 7877–7888, 2025. 5, 1
- [2] Shuai Bai, Keqin Chen, Xuejing Liu, Jialin Wang, Wenbin Ge, Sibao Song, Kai Dang, Peng Wang, Shijie Wang, Jun Tang, et al. Qwen2. 5-vl technical report. *arXiv preprint arXiv:2502.13923*, 2025. 3
- [3] Black Forest Labs. Flux.1 [dev] — model card. <https://huggingface.co/black-forest-labs/FLUX.1-dev>, 2025. 1, 3, 5, 7
- [4] Anthony Chen, Jianjin Xu, Wenzhao Zheng, Gaole Dai, Yida Wang, Renrui Zhang, Haofan Wang, and Shanghang Zhang. Training-free regional prompting for diffusion transformers. *arXiv preprint arXiv:2411.02395*, 2024. 2, 3, 4, 5, 6
- [5] Dar-Yen Chen, Hmrishav Bandyopadhyay, Kai Zou, and Yi-Zhe Song. Normalized attention guidance: Universal negative guidance for diffusion model. *arXiv preprint arXiv:2505.21179*, 2025. 3
- [6] Minghao Chen, Iro Laina, and Andrea Vedaldi. Training-free layout control with cross-attention guidance. In *Proceedings of the IEEE/CVF winter conference on applications of computer vision*, pages 5343–5353, 2024. 3
- [7] Ruidong Chen, Lanjun Wang, Weizhi Nie, Yongdong Zhang, and An-An Liu. Anyscene: Customized image synthesis with composited foreground. In *Proceedings of the IEEE/CVF Conference on Computer Vision and Pattern Recognition*, pages 8724–8733, 2024. 3
- [8] Zhennan Chen, Yajie Li, Haofan Wang, Zhibo Chen, Zhengkai Jiang, Jun Li, Qian Wang, Jian Yang, and Ying Tai. Ragd: Regional-aware diffusion model for text-to-image generation. In *Proceedings of the IEEE/CVF International Conference on Computer Vision*, pages 19331–19341, 2025. 2, 3, 4, 5, 6, 7
- [9] Omer Dahary, Or Patashnik, Kfir Aberman, and Daniel Cohen-Or. Be yourself: Bounded attention for multi-subject text-to-image generation. In *European Conference on Computer Vision*, pages 432–448. Springer, 2024. 3
- [10] Yusuf Dalva, Yijun Li, Qing Liu, Nanxuan Zhao, Jianming Zhang, Zhe Lin, and Pinar Yanardag. Layerfusion: Harmonized multi-layer text-to-image generation with generative priors. *arXiv preprint arXiv:2412.04460*, 2024. 3
- [11] Patrick Esser, Sumith Kulal, Andreas Blattmann, Rahim Entezari, Jonas Müller, Harry Saini, Yam Levi, Dominik Lorenz, Axel Sauer, Frederic Boesel, et al. Scaling rectified flow transformers for high-resolution image synthesis. In *Forty-first International Conference on Machine Learning*, 2024. 2, 3
- [12] Weixi Feng, Wanrong Zhu, Tsu-jui Fu, Varun Jampani, Arjun Akula, Xuehai He, Sugato Basu, Xin Eric Wang, and William Yang Wang. Layoutgpt: Compositional visual planning and generation with large language models. *Advances in Neural Information Processing Systems*, 36:18225–18250, 2023. 2, 3, 4
- [13] Xiefan Guo, Jinlin Liu, Miaomiao Cui, Jiankai Li, Hongyu Yang, and Di Huang. Initno: Boosting text-to-image diffusion models via initial noise optimization. In *Proceedings of the IEEE/CVF Conference on Computer Vision and Pattern Recognition*, pages 9380–9389, 2024. 3
- [14] Runze He, Bo Cheng, Yuhang Ma, Qingxiang Jia, Shanyuan Liu, Ao Ma, Xiaoyu Wu, Liebucha Wu, Dawei Leng, and Yuhui Yin. Plangen: Towards unified layout planning and image generation in auto-regressive vision language models. In *Proceedings of the IEEE/CVF International Conference on Computer Vision*, pages 18143–18154, 2025. 3
- [15] Alec Helbling, Tuna Meral, Benjamin Hoover, Pinar Yanardag, and Polo Chau. Conceptattention: Diffusion transformers learn highly interpretable features. In *International Conference on Machine Learning*, 2025. 3
- [16] Edward J Hu, Yelong Shen, Phillip Wallis, Zeyuan Allen-Zhu, Yuanzhi Li, Shean Wang, Lu Wang, Weizhu Chen, et al. Lora: Low-rank adaptation of large language models. *ICLR*, 1(2):3, 2022. 2
- [17] Junjia Huang, Pengxiang Yan, Jinhang Cai, Jiyang Liu, Zhao Wang, Yitong Wang, Xinglong Wu, and Guanbin Li. Dreamlayer: Simultaneous multi-layer generation via diffusion mode. *arXiv preprint arXiv:2503.12838*, 2025. 3
- [18] Kaiyi Huang, Kaiyue Sun, Enze Xie, Zhenguo Li, and Xihui Liu. T2i-compbench: A comprehensive benchmark for open-world compositional text-to-image generation. *Advances in Neural Information Processing Systems*, 36:78723–78747, 2023. 6, 7, 2, 3
- [19] Yue Jiang, Yueming Lyu, Bo Peng, Wei Wang, and Jing Dong. Cmsl: Cross-modal style learning for few-shot image generation. *Machine Intelligence Research*, 22(4):752–768, 2025. 3
- [20] Dongyang Jin, Ryan Xu, Jianhao Zeng, Rui Lan, Yancheng Bai, Lei Sun, and Xiangxiang Chu. Semantic context matters: Improving conditioning for autoregressive models. *arXiv preprint arXiv:2511.14063*, 2025. 3
- [21] Zeeshan Khan, Shizhe Chen, and Cordelia Schmid. Composeanything: Composite object priors for text-to-image generation. *arXiv preprint arXiv:2505.24086*, 2025. 3, 4, 6, 2
- [22] Chaehyun Kim, Heeseong Shin, Eunbeen Hong, Heeji Yoon, Anurag Arnab, Paul Hongsuck Seo, Sunghwan Hong, and Seungryong Kim. Seg4diff: Unveiling open-vocabulary semantic segmentation in text-to-image diffusion transformers. In *The Thirty-ninth Annual Conference on Neural Information Processing Systems*, 2025. 3
- [23] Daneul Kim, Jaeh Lee, and Jaesik Park. Improving editability in image generation with layer-wise memory. In *Proceedings of the Computer Vision and Pattern Recognition Conference*, pages 7889–7898, 2025. 3
- [24] Yulhwa Kim, Dongwon Jo, Hyesung Jeon, Taesu Kim, Daehyun Ahn, Hyungjun Kim, et al. Leveraging early-stage robustness in diffusion models for efficient and high-quality image synthesis. *Advances in Neural Information Processing Systems*, 36:1229–1244, 2023. 2
- [25] Rui Lan, Yancheng Bai, Xu Duan, Mingxing Li, Dongyang Jin, Ryan Xu, Dong Nie, Lei Sun, and Xiangxiang

- Chu. Flux-text: A simple and advanced diffusion transformer baseline for scene text editing. *arXiv preprint arXiv:2505.03329*, 2025. 3
- [26] Yuseung Lee, Taehoon Yoon, and Minhyuk Sung. Groundit: Grounding diffusion transformers via noisy patch transplantation. *Advances in Neural Information Processing Systems*, 37:58610–58636, 2024. 3
- [27] Yuheng Li, Haotian Liu, Qingyang Wu, Fangzhou Mu, Jianwei Yang, Jianfeng Gao, Chunyuan Li, and Yong Jae Lee. Gligen: Open-set grounded text-to-image generation. In *Proceedings of the IEEE/CVF conference on computer vision and pattern recognition*, pages 22511–22521, 2023. 2, 3, 5, 6, 7
- [28] Dong Liang, Jinyuan Jia, Yuhao Liu, Zhanghan Ke, Hongbo Fu, and Rynson WH Lau. Vodiff: Controlling object visibility order in text-to-image generation. In *Proceedings of the Computer Vision and Pattern Recognition Conference*, pages 18379–18389, 2025. 2, 3
- [29] Zhiqiu Lin, Deepak Pathak, Baiqi Li, Jiayao Li, Xide Xia, Graham Neubig, Pengchuan Zhang, and Deva Ramanan. Evaluating text-to-visual generation with image-to-text generation. *arXiv preprint arXiv:2404.01291*, 2024. 6, 3
- [30] Yaron Lipman, Ricky TQ Chen, Heli Ben-Hamu, Maximilian Nickel, and Matt Le. Flow matching for generative modeling. *arXiv preprint arXiv:2210.02747*, 2022. 2
- [31] Zhengyao Lv, Tianlin Pan, Chenyang Si, Zhaoxi Chen, Wangmeng Zuo, Ziwei Liu, and Kwan-Yee K Wong. Re-thinking cross-modal interaction in multimodal diffusion transformers. In *Proceedings of the IEEE/CVF International Conference on Computer Vision*, 2025. 5, 7, 1
- [32] Jiafeng Mao, Xueting Wang, and Kiyoharu Aizawa. The lottery ticket hypothesis in denoising: Towards semantic-driven initialization. In *European Conference on Computer Vision*, pages 93–109. Springer, 2024. 2, 3
- [33] Ben Mildenhall, Pratul P Srinivasan, Matthew Tancik, Jonathan T Barron, Ravi Ramamoorthi, and Ren Ng. Nerf: Representing scenes as neural radiance fields for view synthesis. *Communications of the ACM*, 65(1):99–106, 2021. 3
- [34] OpenAI. Gpt5 — model card. <https://openai.com/index/gpt-5-system-card/>, 2025. 6, 2
- [35] William Peebles and Saining Xie. Scalable diffusion models with transformers. In *Proceedings of the IEEE/CVF international conference on computer vision*, pages 4195–4205, 2023. 2
- [36] Quynh Phung, Songwei Ge, and Jia-Bin Huang. Grounded text-to-image synthesis with attention refocusing. In *Proceedings of the IEEE/CVF Conference on Computer Vision and Pattern Recognition*, pages 7932–7942, 2024. 2, 3
- [37] Gabriel Raya and Luca Ambrogioni. Spontaneous symmetry breaking in generative diffusion models. *Advances in Neural Information Processing Systems*, 36, 2024. 2
- [38] R. Rombach. Stable diffusion v1-4 model card. model card, 2022. 2, 3
- [39] Stability AI. Stable diffusion 3.5 large — model card. <https://huggingface.co/stabilityai/stable-diffusion-3.5-large>, 2025. 1, 5
- [40] Jianlin Su, Murtadha Ahmed, Yu Lu, Shengfeng Pan, Wen Bo, and Yunfeng Liu. Roformer: Enhanced transformer with rotary position embedding. *Neurocomputing*, 568:127063, 2024. 4
- [41] Petru-Daniel Tudosiu, Yongxin Yang, Shifeng Zhang, Fei Chen, Steven McDonagh, Gerasimos Lampouras, Ignacio Iacobacci, and Sarah Parisot. Mulan: A multi layer annotated dataset for controllable text-to-image generation. In *Proceedings of the IEEE/CVF Conference on Computer Vision and Pattern Recognition*, pages 22413–22422, 2024. 3
- [42] Jiangshan Wang, Junfu Pu, Zhongang Qi, Jiayi Guo, Yue Ma, Nisha Huang, Yuxin Chen, Xiu Li, and Ying Shan. Taming rectified flow for inversion and editing. *arXiv preprint arXiv:2411.04746*, 2024. 8, 4
- [43] Xudong Wang, Trevor Darrell, Sai Saketh Rambhatla, Rohit Girdhar, and Ishan Misra. InstanceDiffusion: Instance-level control for image generation. In *Proceedings of the IEEE/CVF conference on computer vision and pattern recognition*, pages 6232–6242, 2024. 3, 7
- [44] Tianyi Wei, Yifan Zhou, Dongdong Chen, and Xingang Pan. Freeflux: Understanding and exploiting layer-specific roles in rope-based mmdit for versatile image editing. *arXiv preprint arXiv:2503.16153*, 2025. 3, 5, 1
- [45] Keming Wu, Junwen Chen, Zhanhao Liang, Yinuo Wang, Ji Li, Chao Zhang, Bin Wang, and Yuhui Yuan. Hybrid layout control for diffusion transformer: Fewer annotations, superior aesthetics. In *Proceedings of the IEEE/CVF International Conference on Computer Vision*, pages 17930–17940, 2025. 2, 3, 5, 6, 7
- [46] Xiaoshi Wu, Yiming Hao, Keqiang Sun, Yixiong Chen, Feng Zhu, Rui Zhao, and Hongsheng Li. Human preference score v2: A solid benchmark for evaluating human preferences of text-to-image synthesis. *arXiv preprint arXiv:2306.09341*, 2023. 6, 3
- [47] Qiang Xiang, Shuang Sun, Binglei Li, Dejia Song, Huaxia Li, Nemo Chen, Xu Tang, Yao Hu, and Junping Zhang. Instanceassemble: Layout-aware image generation via instance assembling attention. *arXiv preprint arXiv:2509.16691*, 2025. 2, 3, 5, 7, 6
- [48] Ruihang Xu, Dewei Zhou, Fan Ma, and Yi Yang. Contextgen: Contextual layout anchoring for identity-consistent multi-instance generation. *arXiv preprint arXiv:2510.11000*, 2025. 3
- [49] Ling Yang, Zhaochen Yu, Chenlin Meng, Minkai Xu, Stefano Ermon, and Bin Cui. Mastering text-to-image diffusion: Recaptioning, planning, and generating with multimodal llms. In *Forty-first International Conference on Machine Learning*, 2024. 2, 3, 4
- [50] Hu Ye, Jun Zhang, Sibio Liu, Xiao Han, and Wei Yang. Ip-adapt: Text compatible image prompt adapter for text-to-image diffusion models. *arXiv preprint arXiv:2308.06721*, 2023. 5
- [51] Jianhao Zeng, Yancheng Bai, Ruidong Chen, Xuanpu Zhang, Lei Sun, Dongyang Jin, Ryan Xu, Nannan Zhang, Dan Song, and Xiangxiang Chu. Eevee: Towards close-up high-resolution video-based virtual try-on. *arXiv preprint arXiv:2511.18957*, 2025. 3

- [52] Xiaohang Zhan and Dingming Liu. Larender: Training-free occlusion control in image generation via latent rendering. In *Proceedings of the IEEE/CVF International Conference on Computer Vision*, pages 19679–19688, 2025. [1](#), [2](#), [3](#), [5](#), [6](#), [7](#)
- [53] Hui Zhang, Dexiang Hong, Yitong Wang, Jie Shao, Xinglong Wu, Zuxuan Wu, and Yu-Gang Jiang. Creatilayout: Siamese multimodal diffusion transformer for creative layout-to-image generation. In *Proceedings of the IEEE/CVF International Conference on Computer Vision*, pages 18487–18497, 2025. [1](#), [2](#), [3](#), [4](#), [5](#), [6](#), [7](#)
- [54] Hui Zhang, Dexiang Hong, Maoke Yang, Yutao Cheng, Zhao Zhang, Weidong Chen, Jie Shao, Xinglong Wu, Zuxuan Wu, and Yu-Gang Jiang. Creatidesign: A unified multi-conditional diffusion transformer for creative graphic design. In *The Fourteenth International Conference on Learning Representations*, 2026. [7](#), [3](#)
- [55] Lvmin Zhang and Maneesh Agrawala. Transparent image layer diffusion using latent transparency. *arXiv preprint arXiv:2402.17113*, 2024. [3](#)
- [56] Xinchun Zhang, Ling Yang, Guohao Li, Yaqi Cai, Jiakexie, Yong Tang, Yujie Yang, Mengdi Wang, and Bin Cui. Itercomp: Iterative composition-aware feedback learning from model gallery for text-to-image generation. *arXiv preprint arXiv:2410.07171*, 2024. [3](#), [6](#)
- [57] Xuanpu Zhang, Xuesong Niu, Ruidong Chen, Dan Song, Jianhao Zeng, Penghui Du, Haoxiang Cao, Kai Wu, and Anan Liu. Group relative attention guidance for image editing. *arXiv preprint arXiv:2510.24657*, 2025. [3](#)
- [58] Guangcong Zheng, Xianpan Zhou, Xuewei Li, Zhongang Qi, Ying Shan, and Xi Li. Layoutdiffusion: Controllable diffusion model for layout-to-image generation. In *Proceedings of the IEEE/CVF Conference on Computer Vision and Pattern Recognition*, pages 22490–22499, 2023. [2](#), [3](#), [6](#)
- [59] Dewei Zhou, You Li, Fan Ma, Xiaoting Zhang, and Yi Yang. Migc: Multi-instance generation controller for text-to-image synthesis. In *Proceedings of the IEEE/CVF conference on computer vision and pattern recognition*, pages 6818–6828, 2024. [2](#), [3](#)
- [60] Dewei Zhou, Mingwei Li, Zongxin Yang, and Yi Yang. Dreamrenderer: Taming multi-instance attribute control in large-scale text-to-image models. *arXiv preprint arXiv:2503.12885*, 2025. [3](#)
- [61] Dewei Zhou, Ji Xie, Zongxin Yang, and Yi Yang. 3dis-flux: simple and efficient multi-instance generation with dit rendering. *arXiv preprint arXiv:2501.05131*, 2025. [3](#)

Layer-wise Instance Binding for Regional and Occlusion Control in Text-to-Image Diffusion Transformers

Supplementary Material

This supplementary material is organized as follows:

- Sec. A details optional modules of LayerBind, including the vital block selection for the Hard-Binding and the implementation details of the Layer Blending mechanism.
- Sec. B provides detailed introductions of the experimental setup, including the strategy for layout parsing, the dataset construction, and the evaluation metrics.
- Sec. C provides supplementary experiment analyses, including efficiency and further module ablations.
- Sec. D further discusses applications of LayerBind, including the implementation details for composited image editing and its compatibility with external visual adapters.
- Sec. E address the limitations of LayerBind. We showcase representative failure cases and discuss potential solutions for repair.
- Sec. F provides more visualization of generation results.

A. Optional Modules of LayerBind

A.1. Vital Block Selection for Hard-Binding

As discussed in prior work [31], "modality competition" can cause instances to be suppressed by strong background contexts. To address this, we leverage the observation that different DiT blocks exhibit varying sensitivities to text [1, 44]. We suggest that forcing "text-dominant" blocks to focus exclusively on their primary strength (semantic injection) offers a natural, minimally disruptive intervention for instance initialization.

To identify these vital blocks, we empirically analyze attention maps recorded during generation. Using segmentation tools on multiple runs (20 prompts, 5 seeds), we extract foreground masks and calculate the response intensity of foreground tokens (as queries) to different token types, averaged over the first 20% of steps. The results (Fig. 10) reveal a consistent trend in both FLUX and SD3.5: while foreground self-attention remains high across all layers, responses to background versus text tokens diverge significantly. Early blocks are visually dominant, whereas mid-to-late blocks become progressively more text-responsive. Based on these findings, the selection is twofold:

1. We always select Layer 0, uniquely critical for establishing initial semantic binding [1, 44].
2. We select the 2 most text-responsive blocks from early-mid stages and the 6 most text-responsive blocks from late stages.

This empirical selection balances semantic injection strength with maintaining image generation quality. Specif-

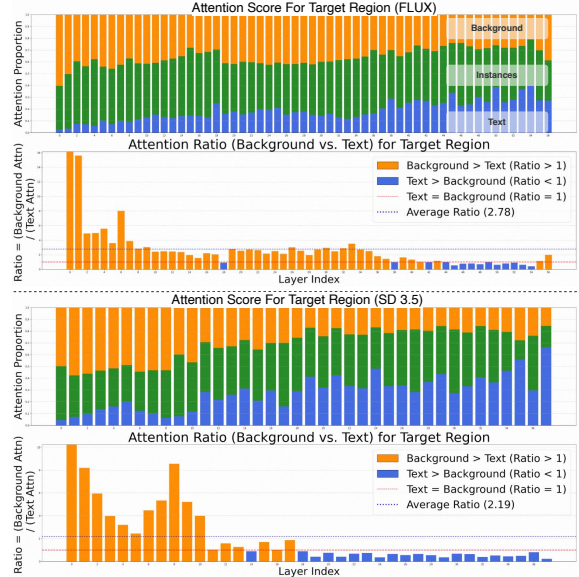


Figure 10. Attention response weights of foreground to background, self, and text tokens across different attention blocks (in FLUX and SD3.5).

ically, we select blocks [0, 15, 18, 42, 45, 48, 50, 53, 54] for FLUX (partially aligning with [1, 44]) and [0, 11, 14, 19, 21, 24, 29, 32, 34] for SD3.5. Restricting Hard Binding to these vital blocks maximizes semantic injection while minimizing disruption to overall quality, as applying it to excessive blocks degrades performance.

A.2. Layer Blending Module

As described in Sec. 4.2, we composite occluding layers using a foreground-aware alpha mask $\alpha^{(i)}$. Since the branch $B^{(i)}$ and global latent I share the same background context, we can estimate this mask directly from their difference. First, we compute a robust saliency map Z by normalizing the difference using the local background variance (σ_{bg}), estimated from the Median Absolute Deviation (MAD) of a surrounding background area with the estimated region:

$$Z = \text{Smooth} \left(\left\| \frac{B^{(i)} - I[idx^{(i)}]}{\sigma_{bg} + \epsilon} \right\|_2^\gamma \right) \quad (13)$$

where $I[idx^{(i)}]$ is the global latent in the instance region and γ is a correction factor, default with 0.9. This coarse saliency map Z is then refined into a spatially smooth alpha mask by solving a Screened Poisson equation via an itera-

tive solver:

$$\alpha_{k+1} = \frac{1}{4 + \lambda} \left(\sum_{p \in \mathcal{N}(\alpha_k)} \alpha_p + \lambda Z \right) \quad (14)$$

where λ balances the data term Z against the smoothness term. After convergence, we apply an optional Otsu’s thresholding (a classic, unsupervised algorithm for automatic foreground thresholding) to explicitly separate the foreground region. Finally, we perform morphological reconstruction to fill any internal holes, ensuring the instance appears contiguous and enhancing the blend’s realism.

B. Extended Evaluation Details

B.1. LLM-based Layout Parser

As outlined in Sec. 4.1, consistent with prior works [8, 21, 49, 53], we employ an LLM to generate layout plans when precise user-specified layouts are unavailable. However, LayerBind has specific input requirements that generic parsers neglect: a decoupled background prompt and an explicit occlusion order. To address this, we design a specialized prompt engineering strategy using a state-of-the-art LLM (e.g., GPT-5-mini [34]), as visualized in Fig. 11. The parsing process leverages Chain-of-Thought (CoT) prompting and is divided into two distinct stages:

1. **Spatial reasoning:** The LLM first engages in a planning phase to analyze the input caption. It deduces the overall scene structure, ensuring logical spatial relationships and reasonable object placement before committing to coordinates.
2. **Structured output:** We constrain the LLM to output a JSON. Crucially, this schema requires the model to explicitly generate a "background_prompt" for context isolation and assign an "order" index to each instance based on its layer index, thereby rigorously defining the occlusion hierarchy.

To ensure stability and adherence to this schema, we utilize in-context learning by providing few-shot examples (as shown at the bottom of Fig. 11), enabling the model to learn the correct patterns for layout generation.

Furthermore, this parser serves as the foundation for our benchmark construction. Although prior works [8, 21, 49, 53] have utilized layout generation for evaluating T2I-CompBench, none have publicly released their ground-truth layout annotations. This absence prevents a fair, unified comparison across different methods. Therefore, we use this standardized parser to re-annotate the dataset, ensuring a consistent evaluation ground for all baselines.

B.2. Dataset Construction

We evaluate LayerBind on two primary tasks: Occlusion Control and General T2I Alignment. Our prompts are primarily sourced from T2I-CompBench [18]. However, as

Layer Parser Prompt (Simplified)

You are a layout annotator for text-to-image generation.
 Goal: From an input text prompt, produce ONLY a JSON object with:

- planning, rewritten prompt,
- background prompt,
- instances list: instances with isolated captions, 1024×1024 bounding boxes, and depth order.

Rules (Detailed rules are attached after each item):

1. Plan the layout: ...
2. Rewrite the caption: ...
3. Instance extraction: ...
4. Generate detailed caption for each instance: ...
5. Relative depth annotation: ...
6. Bounding box layout annotation: ...
7. Generate background prompt for overall scene: ...

Input: <INPUT_PROMPT>
 OUTPUT JSON schema:

```
{
  "planning": "string",
  "rewritten_prompt": "string",
  "background_prompt": "string",
  "elements": [
    {
      "region_prompt": "string",
      "layout": [x_top, y_top, x_bottom, y_bottom],
      "order": 1
    }
  ]
}
```

<In-Context Examples>

Figure 11. The simplified prompt template used for our LLM-based Layout Parser. Specific rules are defined for each part of the parsing, and these rules are made comprehensible to the model through In-Context Examples.

this benchmark lacks publicly available layout annotations, we re-annotated the data using our proposed Layout-Parser to ensure a unified input setting. The dataset construction consists of two parts:

- **Layout-annotated T2I-CompBench:** We utilize the *color*, *shape*, *texture*, *2D-spatial*, *numeracy*, and *complex* subsets for general alignment evaluation. For the 3D-spatial subset, which focuses on occlusion, we applied strict filtering. We employed the Layout-Parser to generate bounding boxes and layer orders, followed by manual verification to remove invalid cases (e.g., where regions are fully occluded or exhibit ambiguous 3D relationships). This resulted in 800 high-quality prompts for occlusion evaluation. The sample counts for other subsets remain consistent with the original benchmark.
- **BindBench (Complex Occlusion):** The original T2I-CompBench-3D is limited to spatial relationships between only two objects, which is insufficient for evaluat-

ing complex occlusion. Notably, LaRender [52] proposed the RealOcc dataset to address similar issues; however, it contains only 60 prompts and is currently not publicly accessible. To enable a more comprehensive evaluation, we construct **BindBench**. We reuse instance categories from T2I-CompBench but recombined them to form complex scenes featuring 3 to 5 overlapping objects. After applying our Layout-Parser for annotation and conducting rigorous manual filtering, we obtain 200 challenging prompts specifically designed to benchmark multi-instance occlusion control.

To comprehensively assess LayerBind’s performance in terms of layout precision, occlusion accuracy, semantic consistency, and generation quality, we employ the following metrics:

B.3. Evaluation Metrics

1. UniDet-Depth (Relative Depth Accuracy). We utilize the official evaluation script from T2I-CompBench [18]. This metric employs the UniDet depth estimation model to predict the depth map of the generated image. It then computes the average depth value within the ground-truth bounding boxes of instance pairs to determine if the generated depth order matches the input condition.

2. CLIP Score (Semantic Alignment). We assess text-image alignment at both global and local levels using the CLIP ViT-L/14 model:

- **CLIP-G (Global Consistency):** We calculate the cosine similarity between the whole image embedding and the full scene text embedding. This measures how well the overall image captures the global prompt, reflecting both object existence and reasonable spatial composition.
- **CLIP-L (Regional Fidelity):** To evaluate whether specific instances are generated with sufficient regional detail, this metric calculates the similarity between the embedding of the cropped instance region (defined by the layout box) and its corresponding regional prompt.

3. $L_{Acc/VQA}$ (Fine-grained Layout Faithfulness). Following [53, 54], which implement VLM-based metrics to evaluate layout faithfulness, we introduce L_{Acc} to measure layout generation accuracy and L_{attr} for fine-grained evaluation of regional attribute fidelity. Both metrics are based on VQAScore [29] and implemented with Qwen2.5-VL [2]. Specifically, L_{Acc} is computed by questioning each region with the template: “This image contains {object class}?”, and L_{attr} is computed by questioning with the detailed regional prompt. These two metrics are evaluated on the more complex BindBench dataset and offer more discriminative comparisons than the CLIP-L.

4. O_{VQA} (Perceptual Occlusion Success). While depth estimation suffices for simple object pairs, it struggles with the complex, multi-instance occlusions found in our BindBench. To address this, we employ the VQAScore [29]



Figure 12. Illustration of leveraging QWen-VL2.5 [2] as a VQA judge for evaluating 3D spatial relationships. It can accurately perceive spatial relationships and score the image content on whether it satisfies the question.

Model	1	2	3	4	5	6
FLUX	18%	31%	45%	60%	76%	89%
SD3.5	24%	39%	55%	73%	92%	107%

Table 4. LayerBind’s additional inference time when inputting different numbers of regions. Each region occupies 25% of the image tokens (e.g., 1024 tokens). The inference cost of LayerBind increases linearly with the number of additional tokens.

as a perceptual metric to develop the O_{VQA} metric. Similar to $L_{Acc/VQA}$, we utilize Qwen2.5-VL [2] as a visual judge. We feed the generated image and a query regarding the occlusion relationship into the MLLM (as illustrated in Fig. 12). The model’s accuracy serves as a proxy for the human-perceived success rate of occlusion control.

5. HPS v2 (Generation Quality). Layout control methods often risk degrading image quality (e.g., introducing unnatural lighting or artifacts). To quantify this trade-off, we report the Human Preference Score v2 (HPS) [46]. Trained on large-scale human choices, HPS correlates well with human aesthetic judgments. A higher HPS indicates that LayerBind effectively preserves the high-fidelity generation capabilities of the base DiT model.

C. Extended Experiment Analysis

C.1. Efficiency Analysis

In terms of run-time efficiency, the introduction of instance branches inevitably increases the total token count, leading to additional computational overhead. In Table 1, we initially reported the inference overhead for standard generation scenarios (based on BindBench cases, involving approximately 40–50% additional tokens). To more comprehensively evaluate LayerBind’s inference efficiency, Table 4 details the overheads of varying loads, ranging from 1 to 6 input regions (corresponding to a token count increase of 25% to 150%). LayerBind’s overhead scales linearly with the number of additional tokens, avoiding the quadratic computational explosion often associated with extended token sequences in Transformers. This efficiency is attributed to two key design choices: (1) branch tokens

are active only during the limited early initialization steps, and (2) our local update calculation employs an block-wise strategy rather than full-sequence calculation. In summary, LayerBind maintains a highly practical trade-off, achieving precise control with manageable computational costs.



Figure 13. The illustration of the effectiveness of the proposed LSN and naive regional prompting [4] strategies. Without layer-wise updates, errors such as concept blending and failure in occlusion control may occur.

C.2. Layer-wise Nursing vs. Regional Prompting

A straightforward alternative to our Layer-wise Semantic Nursing (LSN) is standard regional prompting [4], which injects semantics without explicit layer-wise compositing. We observe that for layouts with spatially disjoint instances (i.e., no complex occlusion), Regional Prompting effectively refines instance details. However, as illustrated in Fig. 13, it fails in two critical scenarios:

- **Concept Blending:** Without the explicit isolation, attention leakage may occur between regions. This can lead to concept blending, where semantics blend across boundaries even without explicit visual overlap.
- **Occlusion Failure:** During the nursing phase, the initialized latent representations often lack sufficiently distinct semantic boundaries to maintain occlusion naturally. Without layer-wise updates to strictly enforce visibility ordering, standard regional prompting fails to ensure that the foreground robustly overwrites the background. Consequently, the pre-established occlusion relationships degrade or vanish in the final output.

Therefore, we conclude that the proposed LSN is a more robust strategy, essential for maintaining both semantic and the correct occlusion order.

C.3. Effect of η_1 and η_2

The selection of η_1 and η_2 is critical for LayerBind’s performance. First, η_1 is the decisive factor for generation success. As illustrated in Fig. 9, an excessively low η_1 fails to impose sufficient spatial constraints, while an overly high value causes significant stylistic or layout over-decoupled between the instance and the background (Fig. 13). As shown in Fig. 14, $\eta_1 = 0.25$ serves as a robust default for both FLUX and SD3.5, though fine-tuning within $[0.1, 0.3]$ can further optimize specific cases. Regarding η_2 , its role includes semantic detail refinement with layout maintenance.

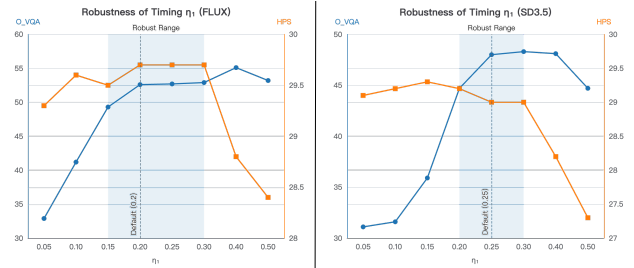


Figure 14. The performance is stabilized across a robust η_1 range, while fine-tuning η_1 can further optimize specific cases.



Figure 15. The visualization of the estimated alpha mask and the effectiveness of different branch blending strategies.

For simple instances where structural preservation is the priority, $\eta_2 = 0.5$ suffices. However, for instances with complex attribute details, we recommend increasing η_2 to 0.7 to ensure faithful semantic details.

C.4. Effectiveness of Branch Blending

The Branch Blending mechanism works as shown in Fig. 15, only applied to the occluded instances region, which is an optional step for enhancing the instance edge quality. We found that in most cases, as long as the bottom-layer instances have sufficient unoccluded parts, direct paste can maintain the occlusion, while further blending strategies further improve the generation quality of both the instances and the overall scene.

D. Extended Applications

D.1. Implementation of Composited Image Editing

As illustrated in Fig. 8, LayerBind supports multi-region, multi-instruction composited image editing. This capability stems from LayerBind’s inherent ability to spawn and merge instance branches onto any arbitrary background generation trajectory. Specifically, the editing pipeline proceeds as follows:

- First, we obtain the denoising trajectory of the image. For synthesized images, we can directly use the original prompt and initial noise; for real images, inversion methods [42] can be used to retrieve the denoising trajectory.
- Then, a key distinction from our standard layout control (which branches at pure noise $t = T$) is the timing of branch creation. For editing tasks, to ensure optimal structural consistency with the original image, we instan-

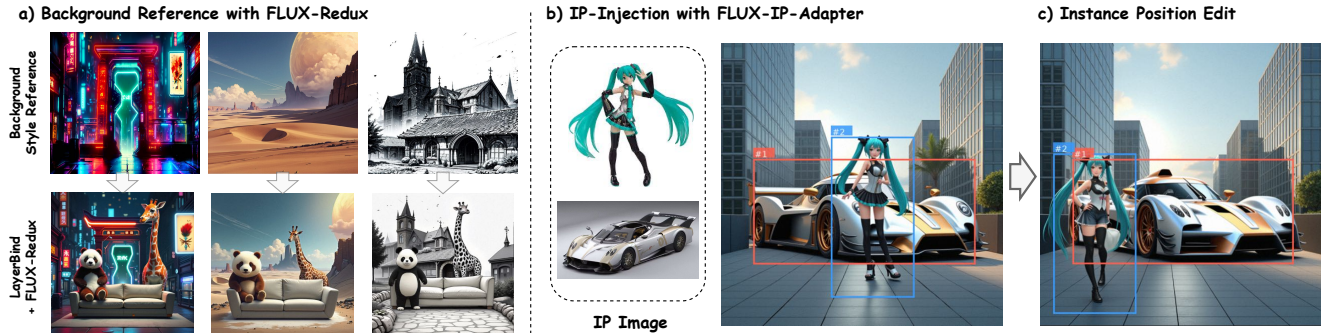


Figure 16. The proposed LayerBind can be integrated with external visual adapters. a) With the FLUX-Redux plugin, LayerBind can directly generate the background by referencing an existing image. b) With IP-adapter [50], LayerBind can inject visual references into regions. c) LayerBind supports instance position editing.

tiate the edit branches after the first denoising step rather than at initialization.

- Finally, each edit region undergoes an independent branch guided by its specific instruction via Eq. 3, functioning analogously to parallel multi-region image inpainting. For fusion, we employ a larger initialization ratio ($\eta_1 \approx 0.4-0.5$). At this stage, the edited content and structure are firmly established; completing the subsequent standard denoising process yields the final edited result.

We plan to provide more extensive analysis and examples of this application in future iterations of this work.

D.2. Compatibility with External Adapters

Since LayerBind relies solely on attention mechanisms, it is inherently compatible with most external adapters. We exemplify this capability in Fig. 16 using two popular tools: the FLUX Redux adapter and IP-Adapter. First, LayerBind can utilize the Redux adapter as a substitute for the textual background prompt. This allows the global scene style to be initialized directly from a reference image while maintaining LayerBind’s structural control. Then, LayerBind integrates seamlessly with IP-Adapter. By injecting visual priors from the IP-Adapter into specific instance regions, LayerBind simultaneously governs both the spatial layout and the specific visual reference.

D.3. Generation with Transparent Instances

Fig. 17 showcases some generation results with transparent instances/reflection, LayerBind can naturally handle transparent object generation without occlusion scenarios. When there is occlusion, since transparent objects are difficult to estimate region alpha using background differences, we directly use direct paste to handle the occluded regions. We found that under the subsequent nursing mechanism, LayerBind can also handle occlusion relationships between transparent instances.



Figure 17. Visualization of generating transparent instances.

D.4. Implementation of Position Editing

As shown in Fig. 16 (c), by making the implementation adjustments, LayerBind can handle instance position editing. The Branch mechanism of LayerBind is built on a shared noisy latent of the regions; therefore, modifying the region coordinates will change the generation trajectory. If it wishes to preserve the originally generated instance features during position editing, alpha estimation should be performed on the instance region before blending it into the new region, rather than directly changing the region coordinates of the instance.

D.5. Complex Scene Generation (>10 Instances)

In Fig. 18, we present the results of using LayerBind to generate more instances of complex layouts. We find that when the input layout itself is spatially logical (i.e., all objects are correctly positioned in the background in a logically reasonable manner), LayerBind is able to accurately handle complex arrangements with more than 10 instances. However, with such a large number of instances, most of the input cases are counterfactual. Since LayerBind is a training-free method that only uses the context sharing ability inherent in the model itself, it struggles to handle generation scenarios outside of its training data distribution, which can lead to artifacts or binding failures.

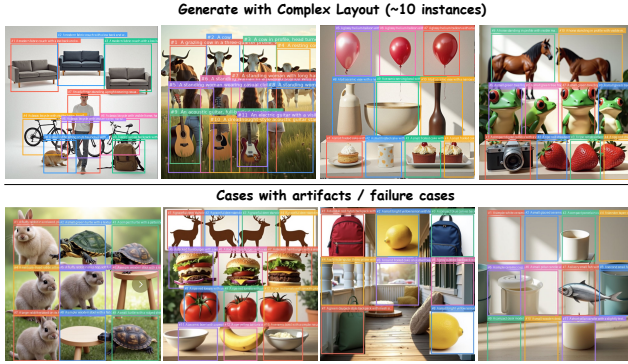


Figure 18. LayerBind successfully handles rational complex spatial relationships, while failing in counterfactually incorrect layout arrangements.

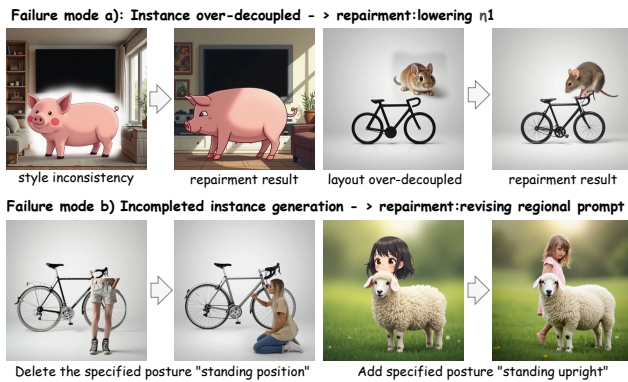


Figure 19. Illustration of typical failure cases and repair measures.

E. Limitations

Fig. 19 illustrates representative failure cases encountered by LayerBind, which can be summarized as follows:

- **Instance-Background over-decoupling:** In some results, we observe a stylistic or structural detachment between the instance and the background. This typically arises when η_1 is set too high, leaving the subsequent nursing phase insufficient capacity to restore global harmony. Reducing η_1 (sacrificing a degree of rigid layout control) effectively mitigates this issue.
- **Incomplete instance generation:** The successful instance generation is dependent on the alignment between its regional prompt and its spatial location. For example, as shown in the figure, depending on the position of the human, adjusting their poses in prompts can avoid incomplete generation.

Beyond the visualized cases, we note that LayerBind struggles with “Dense Layout” scenarios common in traditional Layout-to-Image benchmarks [45, 47, 53, 58]. This limitation stems from our core design: decoupling background and instance generation makes it challeng-

ing to maintain holistic consistency in highly cluttered scenes. Nevertheless, we maintain that LayerBind’s primary strength lies in *customized generation* scenarios as a training-free controller, rather than dense scene synthesis. Future work could explore integrating LayerBind’s mechanics with model fine-tuning strategies to achieve stronger global coherence while retaining precise regional and occlusion control.

F. More Visualizations

Finally, we show cases of more visualization results on the evaluated datasets, in Figs. 20, 21, and 22.

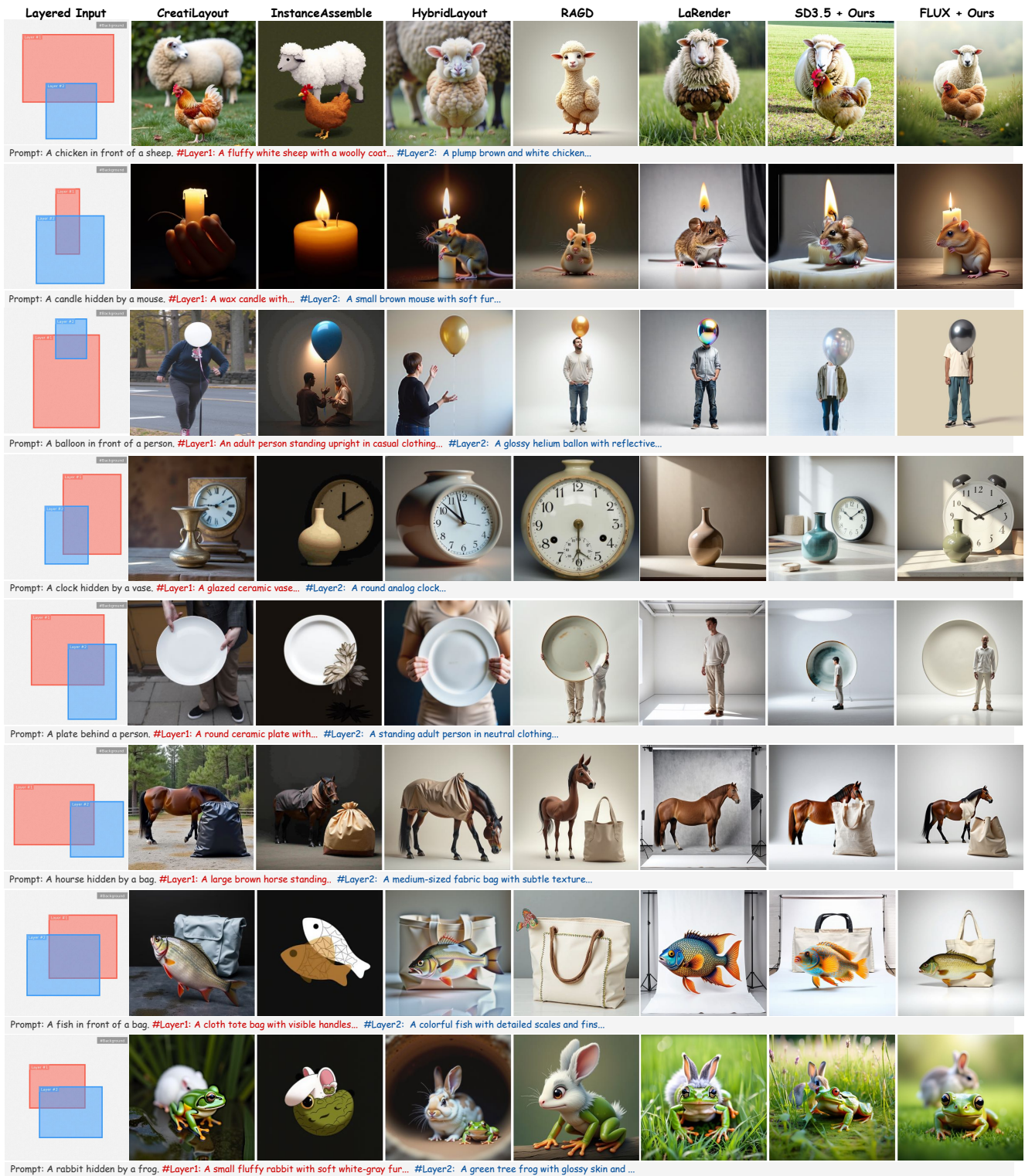


Figure 20. Visualization of occlusion control abilities on T2ICompBench-3D dataset.

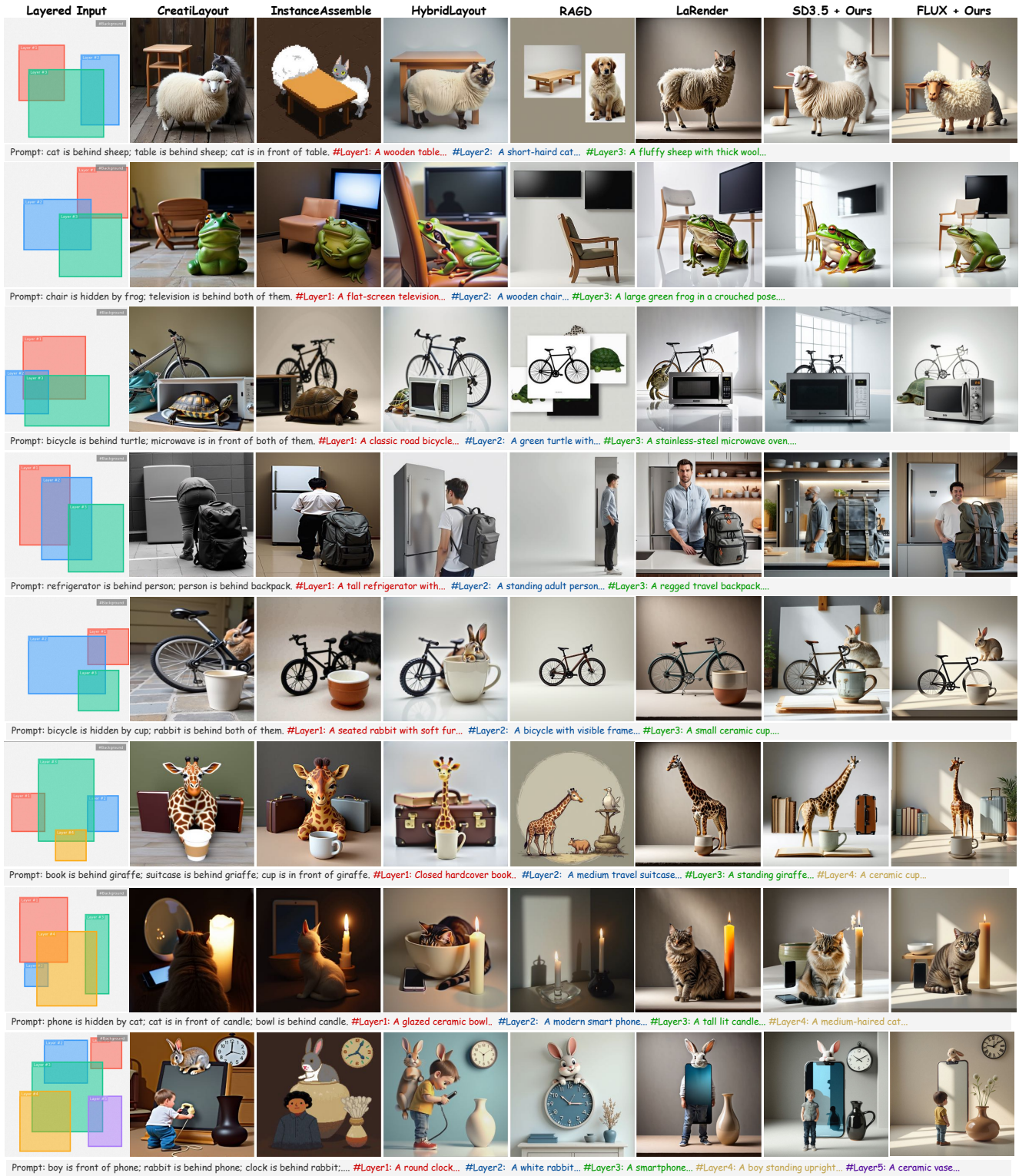


Figure 21. Visualization of occlusion control abilities on BindBench dataset.

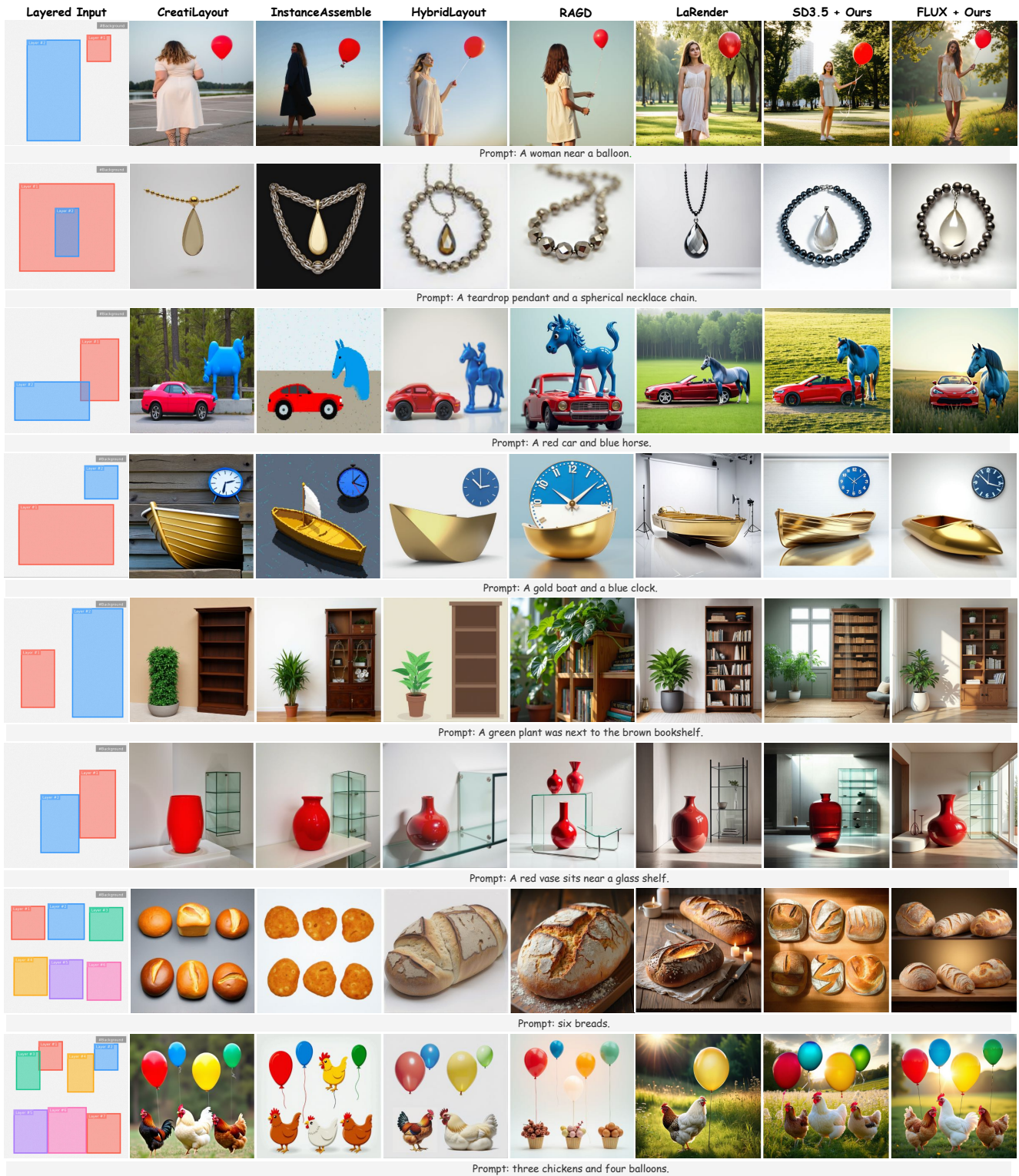


Figure 22. Visualization of T2I alignment tasks on T2ICompBench dataset.